TSSA Journal of Tomography System & Sensors Application Vol. 9, Issue 1, 2026
www.tssa.com.my e-ISSN: 2636-9133

Optimization of Crude Palm Oil Recovery Using a Single-Stage Cartridge Coalescer System

Sauntariya Pandian[1], Nur Tantiyani Ali Othman[1]

[1]Faculty of Engineering & Building Enviroment, Universiti Kebangsaan Malaysia, 43600 UKM Bangi, Selangor, Malaysia

Corresponding author* email: tantiyani@ukm.edu.my
Available online 01 March 2026

ABSTRACT

This study evaluates the limitations of the current two-stage Rapid Tank Crude Palm Oil (CPO) recovery process and proposes a next-generation, single-stage system utilizing cartridge coalescer technology. The primary objective is to minimize oil losses in the underflow, enhance separation efficiency, and develop a more scalable and modular solution tailored for palm oil mill operations. While the existing Rapid Process Flow employed by Sime Darby achieves relatively high CPO recovery, it still suffers from inefficiencies—most notably, significant oil losses in the aqueous underflow, especially under fluctuating feed conditions. Additionally, reliance on multi-stage equipment increases system complexity and capital expenditure. The current setup is not optimized for variable feed characteristics, such as changes in oil concentration or emulsification levels. Furthermore, the absence of a standardized replication framework limits scalability and adaptability. This study introduces an alternative solution designed to address these challenges through a simplified, data-driven, and modular approach.

Keywords: Palm oil recovery, effluent simulation, cartridge coalescer

1. Introduction

Crude Palm Oil (CPO) recovery in palm oil mills is often challenged by fluctuating feed conditions, emulsification, and high equipment complexity in multi-stage separation systems. Sime Darby's current Rapid Process Flow achieves high recovery but still suffers from oil losses in the aqueous underflow (~0.7%), sensitivity to feed variations, and limited scalability. The proposed next-generation single-stage cartridge coalescer aims to simplify operation, reduce oil loss to <0.5%, and provide a modular, adaptable design for mill-wide deployment. The cartridge coalescer employs advanced fiber media to trap fine oil droplets and promote coalescence via wetting, collision, cyclonic, and interception mechanisms, enabling efficient phase disengagement in a compact footprint.

While process simulation in Pro/II can predict bulk phase splits and thermodynamic behaviour, it does not capture spatial maldistribution or interface behaviour inside the vessel—factors critical for achieving the target underflow oil loss. To address this, a SolidWorks-based geometric model of the vessel was integrated with an Electrical Capacitance Tomography (ECT) in-silico module. This approach generates synthetic ECT data from simulated holdup distributions, enabling cross-sectional imaging of oil–water separation patterns without physical sensors. The resulting framework provides both bulk performance metrics and spatial separation insights for design validation and optimization.

2. Electrical Capacitance Tomography

The existing multi-stage CPO recovery system in Sime Darby mills uses a two-stage Rapid Process configuration, consisting of a pre-heating tank, a coalescent tank, and a high-speed separator followed by a vacuum dryer. Separation relies on a combination of gravity settling in the coalescent tank and centrifugal separation in the high-speed separator. This setup delivers relatively high oil recovery but still incurs oil losses in the aqueous underflow of about 0.7%, with a total process time of under two hours. The system is sensitive to changes in feed oil concentration and emulsification, requires moderate maintenance due to multiple pieces of equipment, and is constrained in scalability by tank size and mill layout.

The proposed single-stage cartridge coalescer system consolidates the separation process into a compact vessel containing advanced oleophilic and hydrophobic fiber media that promote rapid droplet coalescence through wetting, collision, cyclonic, and interception mechanisms. This configuration achieves efficient oil–water separation in less than three minutes of residence time, reducing total process time to around 30–45 minutes. Designed for adaptability, it

maintains performance across variable feed conditions while lowering oil loss in the underflow to below 0.5%. The cartridge coalescer is skid-mounted, modular, and easy to install, significantly reducing footprint and complexity compared to the multi-stage system. Maintenance requirements are minimal due to the long service life of the filter media, and environmental compliance is maintained or exceeded through consistently clean aqueous discharge

3. Methodology

The methodology begins with Pro/II process simulations to determine bulk phase splits, densities, viscosities, and compositions under different feed conditions. These results provide the thermodynamic and flow parameters needed for the imaging model. The vessel geometry, including the cartridge coalescer arrangement, is then developed in SolidWorks, producing a 3D model and 2D cross-sections at critical elevations.

From these inputs, an ECT phantom is generated by mapping Pro/II-predicted phase fractions onto the vessel cross-section and assigning each phase its corresponding relative permittivity value. The forward problem is solved using the finite element method (FEM), simulating capacitance measurements for 24 virtual electrodes placed around the vessel wall, with Gaussian noise added to mimic real-world conditions.

The inverse problem is then addressed using a Total Variation (TV) regularized iterative reconstruction algorithm to produce cross-sectional permittivity maps, representing the spatial oil–water holdup distribution. Finally, the reconstructed images are compared to the phantom "ground truth" to assess accuracy, using metrics such as Root Mean Square Error (RMSE), Structural Similarity Index (SSIM), and maldistribution factor. This combined approach allows both bulk and spatial performance evaluation of the cartridge coalescer before physical testing.

4. Results and Discussion

The performance of the proposed single-stage cartridge coalescer system was evaluated through a combination of Pro/II process simulations and in-silico Electrical Capacitance Tomography (ECT) imaging. These tools provided both bulk separation metrics and spatial insights into oil–water holdup distribution under varying feed conditions.

Pro/II simulations demonstrated that the cartridge coalescer consistently achieved underflow oil losses below the target threshold of 0.5% across a wide range of feed compositions. For oil-rich feeds, underflow losses were the lowest, ranging from 0.42% at 5% free fatty acid (FFA) content to 0.45% at 14% FFA. In contrast, water-rich feeds exhibited slightly higher losses, between 0.46% and 0.48%. This increase is attributed to reduced oil residence time and enhanced emulsion stability due to higher aqueous content.

A clear trend was observed where increasing FFA content negatively impacted separation efficiency. This aligns with the known role of FFAs in stabilizing emulsions, which hinders droplet coalescence and settling. These findings validate the cartridge coalescer's capability to maintain high recovery efficiency, even under challenging feed conditions.

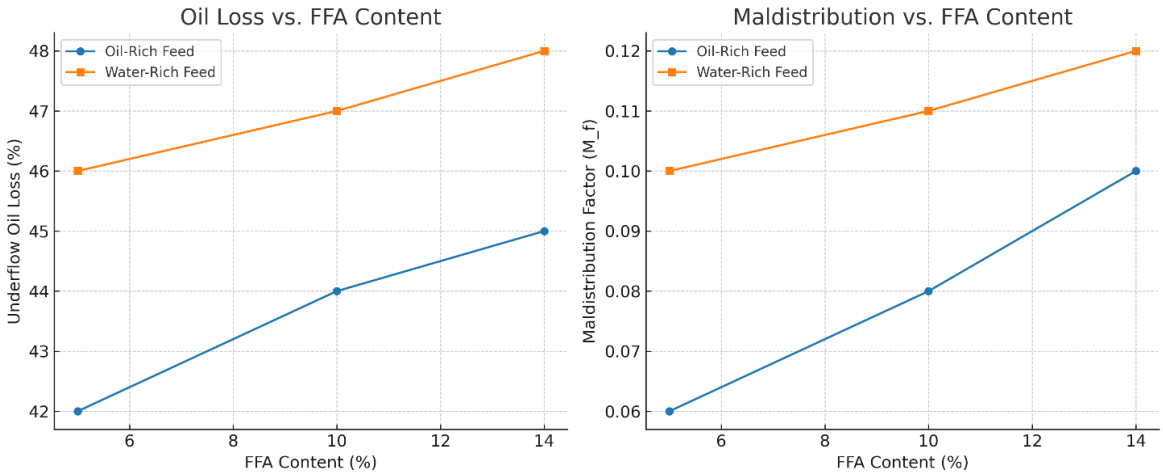

Figure 1. Trends of underflow oil loss (%) and Maldistribution Factor vs the FFA Content

To complement the bulk simulations, ECT-based in-silico imaging was employed to assess internal flow behavior and holdup distribution. The reconstructed permittivity maps revealed that oil-rich feeds maintained relatively uniform holdup profiles, with maldistribution factors (Mf) ranging from 0.06 to 0.10. Conversely, water-rich feeds, particularly

those with high FFA content, exhibited more pronounced concentration zones near the inlet region. In these cases, Mf values increased to approximately 0.12, indicating uneven cartridge loading and tilted interface profiles in the boot section.

These spatial variations directly correlated with the underflow oil losses observed in the Pro/II simulations. The results suggest that maldistribution within the vessel contributes to performance degradation, especially under high-FFA, water-rich conditions.

The analysis highlights the importance of feed composition in determining the coalescer's performance. While the current design performs optimally with oil-rich and balanced feeds, its efficiency approaches the design limit under water-rich, high-FFA scenarios. To address this, targeted design enhancements—such as incorporating flow conditioning inlets or implementing feed preheating—are recommended. These modifications could improve holdup uniformity, reduce maldistribution, and further lower underflow oil losses.

The integration of bulk and spatial simulation tools provides a robust framework for evaluating and optimizing the coalescer design prior to physical implementation. This approach not only reduces development time and cost but also ensures that the system is tailored to real-world operating conditions

5. Conclusions

This study demonstrates that the proposed single-stage cartridge coalescer can achieve the target underflow oil loss of <0.5% across a range of feed compositions, while offering a compact, modular, and operationally flexible alternative to conventional multi-stage separation systems. Bulk Pro/II simulations confirmed strong performance for oil-rich and balanced feeds, with predicted underflow losses as low as 0.42%. Water-rich, high-FFA feeds exhibited slightly higher losses, approaching 0.48%, highlighting the influence of feed composition on separation efficiency.

The integration of in-silico Electrical Capacitance Tomography (ECT) into the evaluation process provided critical spatial performance insights, revealing that maldistribution factors remained low (<0.06) in oil-rich feeds but increased to ~0.12 in challenging water-rich, high-FFA conditions. These elevated maldistribution values correlated directly with higher oil losses, indicating that uneven cartridge loading and interface instability can limit performance in certain operating scenarios.

Overall, the combined simulation and imaging framework proves effective for linking bulk efficiency predictions to internal flow and holdup patterns, enabling informed design adjustments before fabrication. The results suggest that while the current configuration meets its primary performance targets, further optimizations such as inlet flow conditioning or feed heating—could enhance robustness under the most demanding feed conditions. This methodology offers a replicable, low-cost approach for process design, optimization, and scale-up in the palm oil industry and can be extended to other two-phase separation applications.

Acknowledgment

This research is fully supported by GUP-2024-061 grant and FRGS grant, FRGS/1/2024/TK05/UKM/02/4. The authors fully acknowledge the Ministry of Higher Education (MOHE) and Universiti Kebangsaan Malaysia for the approved fund which makes this important research viable and effective.

References

[1] W. Deabes and K. E. Bouazza, "Efficient Image Reconstruction Algorithm for ECT System Using Local Ensemble Transform Kalman Filter," *IEEE Access*, vol. 9, pp. 12779–12790, 2021, doi: 10.1109/ACCESS.2021.3051560.

[2] N. A. A. Rahman *et al.*, "A review on electrical capacitance tomography sensor development," *Jurnal Teknologi*, vol. 73, no. 3, pp. 35–41, 2015, doi: 10.11113/jt.v73.4244.

[3] R. Abdul Rahim, *Electrical capacitance Tomography; Principles, Techniques and Applications*. Penerbit UTM Press, 2011.

[4] Y. Xu, H. Pu, Y. Li, and H. Wang, "Flow pattern identification for gas-oil two-phase flow based on a virtual capacitance tomography sensor and numerical simulation," *Flow Measurement and Instrumentation*, vol. 92, no. March, 2023, doi: 10.1016/j.flowmeasinst.2023.102376.

[5] R. K. Rasel, S. M. Chowdhury, Q. M. Marashdeh, and F. L. Teixeira, "Review of Selected Advances in Electrical Capacitance Volume Tomography for Multiphase Flow Monitoring," *Energies*, vol. 15, no. 14, pp. 1–22, 2022, doi: 10.3390/en15145285.

[6] A. J. Roman, J. S. Ervin, and J. Cronin, "Studies of two-phase flow through a sudden expansion using electrical capacitance tomography," *International Journal of Refrigeration*, vol. 119, pp. 206–215, 2020, doi: 10.1016/j.ijrefrig.2020.07.002.

[7] W. Deabes, A. Sheta, K. E. Bouazza, and M. Abdelrahman, "Application of electrical capacitance tomography for imaging conductive materials in industrial processes," *Journal of Sensors*, vol. 2019, no. ii, 2019, doi: 10.1155/2019/4208349.

[8] N. Ishak, C. K. Lee, and S. Z. Mohd Muji, "A Simulation Magnetic Induction Tomography (MIT) for Agarwood using COMSOL Multiphysics," *International Journal of Engineering and Advanced Technology*, vol. 10, no. 3, pp. 67–71, 2021, doi: 10.35940/ijeat.c2174.0210321.

[9] M. H. Fazalul Rahiman and S. P. Jack, *Microwave Tomography For Agarwood Detection*. Universiti Malaysia Perlis, Malaysia., 2021.

[10] B. Liu, C. Tang, K. Tang, and H. Hu, "A Water fraction measurement method using heuristic-Algorithm-based electrical capacitance tomography images post-processing technology," *IEEE Access*, vol. 8, no. 1, pp. 206418–206426, 2020, doi: 10.1109/ACCESS.2020.3037721.

[11] P. Kalarickel Ramakrishnan *et al.*, "Capacitance Estimation for Electrical Capacitance Tomography Sensors Using Digital Processing of Time-Domain Voltage Response to Single-Pulse Excitation," *Electronics (Switzerland)*, vol. 12, no. 15, 2023, doi: 10.3390/electronics12153242.

[12] M. A. Rodriguez Frias and W. Yang, "Dual-modality four-wire electrical capacitance and resistance tomography," *IST 2018 - IEEE International Conference on Imaging Systems and Techniques, Proceedings*, pp. 1–5, 2018, doi: 10.1109/IST.2018.8577174.

[13] M. Faris, A. Hisham, Y. A. Wahab, Z. Zain, M. Hafiz, and F. Rahiman, "Does Parallel Projection is Suitable in Electrical Capacitance Tomography ? – A Comparison with Common Approach," *Journal of Tomography System & Sensors Application*, vol. 4, no. 1, pp. 85–92, 2021.

[14] A. E. Che Man *et al.*, "Simulation of frequency selection for invasive approach of electrical capacitance tomography for conducting pipe application using oil-gas regimes," in *Engineering Technology International Conference (ETIC 2022)*, 2023, pp. 63–68, doi: 10.1049/icp.2022.2571.

[15] F. T. Ulaby, E. Michielssen, and U. Ravaioli, *Fundamentals of Applied Electromagnetics*, 6th ed. USA: Pearson, 2010.

[16] H. Herdian, I. Muttakin, A. Saputra, A. Yusuf, W. Widada, and W. P. Taruno, "Hardware implementation of linear back-projection algorithm for capacitance tomography," *Proceedings - 2015 4th International Conference on Instrumentation, Communications, Information Technology and Biomedical Engineering, ICICI-BME 2015*, no. 3, pp. 124–129, 2016, doi: 10.1109/ICICI-BME.2015.7401348.

[17] L. Zhang, Y. Zhai, X. Wang, and P. Tian, "Reconstruction method of electrical capacitance tomography based on wavelet fusion," *Measurement*, vol. 126, no. September 2017, pp. 223–230, 2018, doi: 10.1016/j.measurement.2018.05.006.

[18] Z. Wang, "Applications of objective image quality assessment methods," *Signal Processing Magazine, IEEE*, vol. 28, no. 6, pp. 137–142, 2011, doi: 10.1109/MSP.2011.942295.

[19] Z. Wang and A. C. Bovik, "Error : Love It or Leave It ?," *IEEE Signal Processing Magazine*, vol. 26, no. January, pp. 98–117, 2009.

[20] Z. Wang, A. C. Bovik, H. R. Sheikh, and E. P. Simmoncelli, "Image Quality Assessment: From Error Visibility to Structural Similarity," *IEEE Transactions on Image Processing*, vol. 13, no. 4, pp. 600–612, 2004.